JOURNAL OF GUIDANCE, CONTROL, AND DYNAMICS
Vol. 17, No. 3, May–June 1994

Pointing Control and Vibration Suppression of a Slewing Flexible Frame

Donald J. Leo*
State University of New York at Buffalo, Buffalo, New York 14260
and
Daniel J. Inman†
Virginia Polytechnic Institute and State University, Blacksburg, Virginia 24061

An analytical and experimental control system design for a slewing frame containing active members is presented. This testbed is a model for the slewing of dynamically complex structures such as solar arrays and space trusses. Two of the frame's passive members are replaced by active elements that contain piezoceramic material. The active members are integral in suppressing vibrations because the torsional vibrations are difficult to control with the slewing actuator. The design is performed with a finite element-based model that contains significant error; therefore, both control loops must have performance and stability robustness. Suppression of the torsional motion is accomplished with an active member in a positive position feedback (PPF) loop designed with frequency domain and Nyquist techniques. The pointing controller is designed using μ synthesis to maximize the robustness of the control law. This compensator slews the structure with a two second settling time, 7% overshoot, and less than a 2% steady-state error due to static friction. With the supplementary PPF control loop closed, the settling time of the torsional vibrations is reduced from over 30 s to approximately 6 s. Thus, vibration suppression and satisfactory step response is obtained using robust control laws in multiple feedback loops.

Introduction

SLEWING a flexible structure involves vibration suppression as well as accurate pointing and tracking. For simple structures such as flexible beams, both of these objectives can be obtained using a feedback loop consisting of the slewing actuator and angular rate and position sensors.[1] A variety of control laws have been presented, some based on optimal control theory,[2] others designed with Lyapunov methods.[3] For a structure that exhibits more complicated dynamics, slewing the structure and suppressing vibrations calls for a more sophisticated control system. The increase in controller complexity is necessary as it is likely that not all of the flexible modes are easily controlled using the slewing actuator. A straightforward approach is to take advantage of recent developments in smart structure control and integrate active members into the slewing structure. Integrating active members into the structure provides additional sensors and actuators for feedback control. Vibration suppression and accurate pointing is then accomplished using two separate control loops. The first uses the active members as colocated sensors and actuators to suppress certain flexible modes. A second feedback loop is then designed to slew the structure and satisfy pointing and tracking requirements.

This approach is taken in the design of a control system for a slewing flexible frame. This is a challenging control problem since the slewing motion excites bending and torsional vibrations in the structure. Previous results illustrate the need for multiple control loops, because the torsional motion is difficult to suppress with the slewing actuator.[4] The ability to implement multiple-input-multiple-output (MIMO) control is provided by replacing two passive members of the frame with active elements. The active members can be used in conjunction with the slewing actuator in noncolocated control loops, but simulations indicate that using them as colocated sensor/actuators is more robust.[5] This paper provides a detailed overview of the design of the control system for the slewing flexible frame, with the emphasis on robust controller design and experimental implementation. Although the design is presented specifically for a slewing frame, the techniques can be applied to a wide class of slewing control problems.

Received Feb. 16, 1993, revision received Aug. 10, 1993; accepted for publication Sept. 7, 1993.

*Research Assistant.

†Samuel Herrick Professor, Department of Engineering Science and Mechanics.

Modeling of the Slewing Frame

The slewing frame is modeled as a set of second-order ordinary differential equations of the form

$$\boldsymbol{M}\begin{Bmatrix}\ddot{\boldsymbol{r}}(t)\\ \ddot{\theta}(t)\end{Bmatrix} + \boldsymbol{D}\begin{Bmatrix}\dot{\boldsymbol{r}}(t)\\ \dot{\theta}(t)\end{Bmatrix} + \boldsymbol{K}\begin{Bmatrix}\boldsymbol{r}(t)\\ \theta(t)\end{Bmatrix} = \boldsymbol{B}_m i_a(t) + \sum_{i=1}^{2} \boldsymbol{B}_{pzi} v_{ai}(t) \tag{1}$$

where $\boldsymbol{M}$, $\boldsymbol{D}$, and $\boldsymbol{K}$ are, respectively, the $(n+1)\times(n+1)$ mass, damping, and stiffness matrices derived from a finite-element model consisting of the first n elastic modes of the frame. The modal coordinates are denoted $\boldsymbol{r}(t)$ and the rotation of the structure's rigid body about its axis is $\theta(t)$. The overdot represents differentiation with respect to time. Three inputs to the system exist: the slewing actuator and two active members. The $(n+1)\times 1$ forcing vectors for these actuators are $\boldsymbol{B}_m$, $\boldsymbol{B}_{pz1}$, and $\boldsymbol{B}_{pz2}$, respectively. The slewing actuator is a DC motor with armature current $i_a(t)$, and v_{a1} and v_{a2} are the actuator voltages across the active members. The input to the motor is the armature voltage, $e_a(t)$. The relationship between the input voltage and the armature current is

$$L_a \frac{\mathrm{d}}{\mathrm{d}t}[i_a(t)] + R_a i_a(t) = -K_b \dot{\theta}_s(t) + e_a(t) \tag{2}$$

The parameters L_a and R_a are the inductance and resistance of the DC motor, respectively, and K_b is the back-emf constant. The angular rate of the slewing frame is denoted $\dot{\theta}_s(t)$. It differs

from $\dot{\theta}(t)$ because it is the summation of the rigid body rotation and the rotation due to flexibility. The sensor outputs of the system are the angular rate and position of the frame, $\dot{\theta}_s(t)$ and $\theta_s(t)$, and the output signals of the active members, $v_{pz1}(t)$ and $v_{pz2}(t)$. The outputs are related to the system coordinates and inputs by the expressions

$$\theta_s(t) = \boldsymbol{C}_p \begin{Bmatrix} \boldsymbol{r}(t) \\ \theta(t) \end{Bmatrix} \qquad \dot{\theta}_s(t) = \boldsymbol{C}_v \begin{Bmatrix} \dot{\boldsymbol{r}}(t) \\ \dot{\theta}(t) \end{Bmatrix}$$

$$v_{pz1}(t) = \boldsymbol{B}_{pz1}^T \begin{Bmatrix} \boldsymbol{r}(t) \\ \theta(t) \end{Bmatrix} + K_{fd1} v_{a1}(t) \tag{3}$$

$$v_{pz2}(t) = \boldsymbol{B}_{pz2}^T \begin{Bmatrix} \boldsymbol{r}(t) \\ \theta(t) \end{Bmatrix} + K_{fd2} v_{a2}(t)$$

where $\boldsymbol{C}_p$ and $\boldsymbol{C}_v$ are the $1 \times (n+1)$ output vectors corresponding to the angular position and rate, respectively. Since each active member is a colocated sensor/actuator, the output vector is simply the transpose of the input vector. The impedance mismatch between the active members and the structure is modeled as a feedthrough term K_{fdi}, coupling the output directly to the input. The piezoceramics on the active members are connected to ground through a resistor, thus creating a high-pass filter. The sensor signals from the active members $v_{si}(t)$ and $v_{s2}(t)$ are related to actuator voltages $v_{pz1}(t)$ and $v_{pz2}(t)$ by the following expression:

$$V_{si}(s) = [\tau_s s/(\tau_s s + 1)]\, V_{pzi}(s) = G_{hp}(s) V_{pzi}(s) \tag{4}$$

where s is the Laplace operator and τ_s is the circuit's time constant. The model is displayed graphically in Fig. 1, where the following notation is used:

$$G_m(s) = [1/(L_a s + R_a)] \qquad G_{\text{struc}}(s) = [\boldsymbol{M}s^2 + \boldsymbol{D}s + \boldsymbol{K}]^{-1} \tag{5}$$

The nominal model is based on a 20-mode, finite-element analysis of the flexible frame. The actual values of the motor inductance and resistance are found and used in the model. The time constant of the piezoceramic circuit is measured, and the feedthrough K_{fd} is estimated by comparing the actual transfer function with its experimental counterpart.

Theoretical Considerations

The control system for the smart slewing frame consists of the slewing actuator, angular rate and position sensors, and the active members. To satisfy pointing requirements and simultaneously suppress vibrations, a MIMO control system is implemented. One method of achieving the objectives would be to use MIMO control strategies to design a compensator that suppresses vibrations and slews the frame. This is a systematic approach to the problem, but might become overly conservative in an attempt to satisfy both objectives. Another approach is to first design a controller that adds damping to the structure in certain critical modes, and then use a second feedback loop to slew the frame. The advantage in this method is that the compensators are designed separately, allowing the two objectives to be satisfied independently of one another. Since the model is likely to contain an error, it is important that both control loops maintain stability and performance in the presence of model uncertainty. For this reason, a robustness analysis of the design is performed using the structured singular value test, also called μ analysis.

Vibration Suppression

The first step in the control design is to augment the damping in certain modes through the use of the active members in colocated feedback loops. Since robustness is a priority and a strain signal is available, positive position feedback (PPF) is chosen as the control law. This type of feedback is insensitive to the high-frequency dynamics of the structure, due to the roll off of the compensator.[6] The properties of PPF control give it inherent stability robustness, making it an attractive way of adding damping to a structure. To obtain the stability condition for a single-input-single output (SISO) system, consider the form for the PPF controller,

$$K_{ppf}(s) = \sum_{i=1}^{N_f} \frac{g_{fi}\omega_{fi}^2}{s^2 + 2\zeta_{fi}\omega_{fi}s + \omega_{fi}^2} \tag{6}$$

where g_{fi}, ζ_{fi}, and ω_{fi} are the filter design parameters, and N_f represents the number of filters in the controller. In the ideal case of perfectly colocated control, a Nyquist analysis reveals that an encirclement of (1,0) in the complex plane only occurs at $\omega = 0$, where $s = j\omega$. Thus, the stability is governed by the inequality

$$|K_{ppf}(0) G_{ol}(0)| < 1 \tag{7}$$

where $G_{ol}(s)$ is the open-loop transfer function between the actuator and its colocated sensor. Combining Eqs. (6) and (7) yields

$$|G_{ol}(0)| \sum_{i=1}^{N_f} g_{fi} < 1 \tag{8}$$

The open-loop gain of the SISO transfer function can easily be obtained from frequency response data. The stability condition, Eq. (8), is only valid in the case where no sensor or actuator dynamics exist in the bandwidth of the controller. If these dynamics are present, Eq. (8) is modified in a straightforward manner.

Pointing Control

Once vibration suppression has been achieved, a feedback loop is then designed to slew the frame. Robustness of the

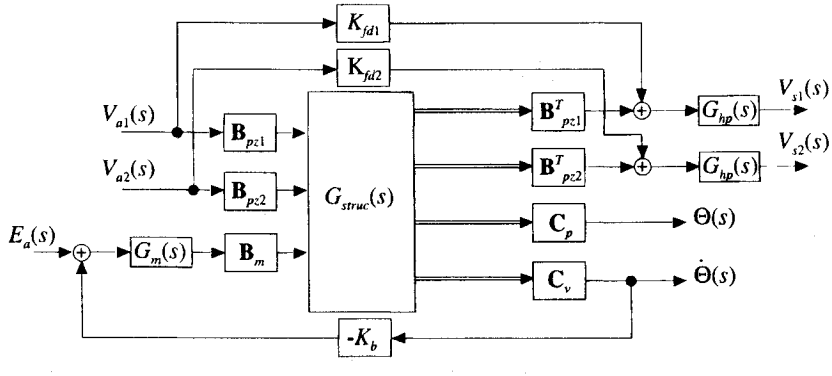

Fig. 1 Block diagram of the slewing frame model.

control law is examined using the structured singular value test, also called μ analysis. To perform μ analysis, the system described in Fig. 1 must be transformed into the block diagram shown in Fig. 2.

The transfer function matrix of the system, with the PPF control loop closed, is denoted $P(s)$. The compensator for pointing control is $K(s)$, and the uncertainty in the system is denoted Δ_u. This transfer function matrix contains the uncertainty descriptions and the performance weights that shape the closed loop. The inputs u_i and outputs y_j are all vector quantities. Closing the feedback loop results in the system $M(s)$. The notation in Fig. 2 indicates that the closed-loop system is a function of $P(s)$ and $K(s)$. Casting the problem into the form shown in Fig. 2 allows for straightforward performance and stability analysis. Three structured singular value tests must be met to achieve nominal and robust performance, as well as robust stability.[7] These are

$$\begin{aligned} &\text{Nominal Performance:} && \mu[M_{22}(s)] < 1 \\ &\text{Robust Stability:} && \mu[M_{11}(s)] < 1 \\ &\text{Robust Performance:} && \mu[M(s)] < 1 \end{aligned} \tag{9}$$

where the $M_{ij}(s)$ is the transfer function matrix between the jth input and the ith output. The maximum structured singular value of a complex matrix μ is a measure of the robustness. Lower values of μ indicate that a design is more robust, hence, one objective is to find a compensator that minimizes the maximum structured singular value.[7] As a design tool, these tests are effective since μ plots can be computed easily and displayed graphically.[8] Inspection of the plots indicates whether performance and stability conditions have been met.

Control System Design for the Slewing Frame

The primary objective of this paper is to design an active control system for a slewing frame. A schematic of the slewing frame testbed is shown in Fig. 3. It consists of a planar frame structure constructed from thin-walled circular aluminum tubing slewed by an Electrocraft 670 DC motor. Two of the members have been replaced by active elements that are flat aluminum bars layered with piezoceramic material. The material is model G-1195 from Piezo Products with dimensions 2.5 × 0.75 × 0.01 in. Each side of an active member has four individual piezoceramic strips bonded to the surface. The four piezoceramics on one side of the member are used to apply a moment to the structure, and the piezoceramics on the opposite side are used as sensors. A more detailed description of the testbed is presented in Leo and Inman.[5]

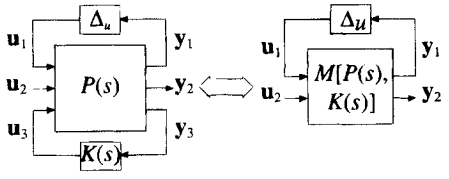

Fig. 2 Block diagram for robust analysis; all inputs and outputs are considered multivariable.

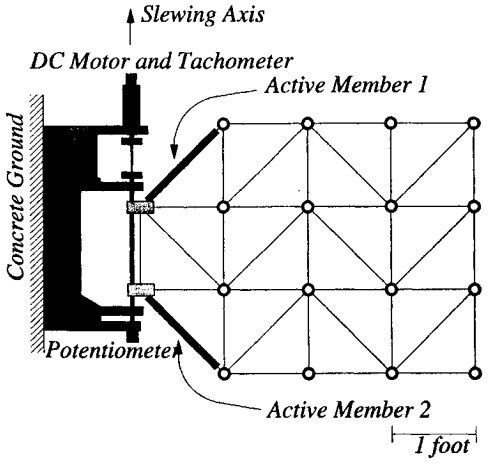

Fig. 3 Schematic of the slewing frame testbed showing the location of the active members, the DC motor, and the angular rate and position sensors.

The validity of the nominal model is assessed by acquiring transfer functions of the slewing frame testbed. Frequency responses are obtained by exciting the structure with either the motor or the active member and measuring the corresponding sensor output. Data acquisition and frequency analysis is performed with a Tektronix 2630 Fourier Analyzer.

Two particular transfer functions are pertinent to the control system design. The first is the output of the tachometer to an input into the slewing actuator, and the second is the transfer function between the actuator on active member 2 and its colocated sensor (Fig. 4). In the case of the tachometer output, the model is accurate over the low frequencies but is in error at the higher frequencies. The nominal model for the colocated sensor/actuator is in better agreement with the actual transfer function. In both magnitude plots, slight variations occur due to the error in the natural frequencies (Table 1), but the overall frequency responses are similar. The damping in the first bending mode of the frame is due to the static friction in the motor and the bearings (Fig. 4a). In the colocated transfer function (Fig. 4b), a resonance at the first clamped-free mode (≃ 11 rad/s) is observed since the moment applied by the active mem-

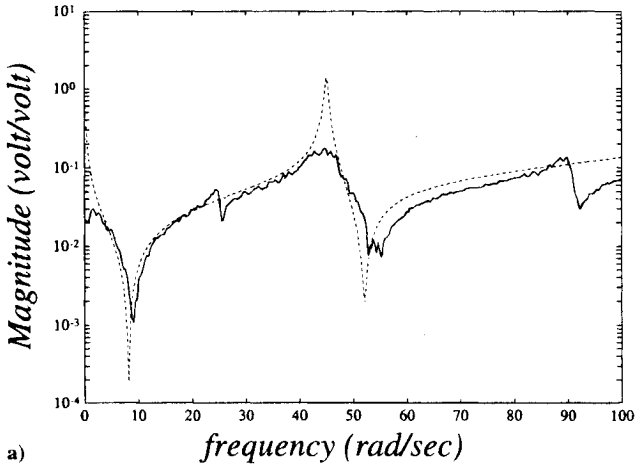

Fig. 4 Comparison between experimental (solid) and analytical (dotted) transfer functions: a) tachometer output/motor input and b) active member 2 output/active member 2 input.

Table 1 Comparison of the first three natural frequencies (in rad/s) of the slewing frame with the values obtained from the nominal model

	Nominal	Exp.
1st torsional	26.43	24.93
1st bending	45.03	44.71
2nd torsional	87.29	89.43

ber is small. This flexible mode is not present during a slewing maneuver, when the frame acts as a pinned-free structure.[5]

Performance for the slewing frame is measured in terms of both step response and vibration suppression. The primary action is to slew the structure using a constant reference input. Because of the frame's flexibility, bending and torsional modes are excited during a slewing maneuver. The distinctive feature of the slewing frame is that the torsional motion is difficult to suppress with the slewing actuator, introducing the need for additional sensors and actuators. The necessary actuators and sensors are obtained by integrating the active members into the slewing frame.

Design of the Positive Position Feedback Filter

The problem of suppressing vibrations during and after the slewing maneuver is directly related to damping the torsional motion of the frame. Initial experiments illustrated the difficulty in suppressing these vibrations with the slewing actuator, hence the need for the active members.[4]

Designing the PPF controller involves choosing the parameters for the second-order filters. Since only one mode is targeted for suppression, only a single filter is necessary [$N_f = 1$ in Eq. (6)]. In this case, three parameters need to be chosen: the filter frequency, gain, and damping ratio. Following the design strategy of Fanson and Caughey,[9] the filter frequency is chosen to be slightly greater than the natural frequency of the first torsional mode and the damping ratio is set in the range of 0.05–0.20. Iteration on the design results in the values $\omega_f = 31$ rad/s and $\zeta_f = 0.10$. The nominal stability of the PPF controller is given by Eq. (8), but a direct application of this expression results in an erroneous stability margin. Due to the presence of the high-pass filter in the open loop, the DC gain of the transfer function is near to zero, resulting in an unrealistically high gain margin. The actual gain margin of the system is determined by a Nyquist analysis of the open-loop system $K_{PPF}(s)\, G_{ol}(s)$. Because of the phase lead that accompanies the high-pass filter, the stability is determined not by the DC gain of the system, but the gain at a frequency of approximately 20 rad/s (Figs. 5a and 5b). A Nyquist plot reveals that the gain corresponding to instability is approximately 2.52. This illustrates that although the actual gain at which instability occurs is much lower than the nominal value, the stability margin is still determined by the low-frequency dynamics of the frame. This is important since in the low-frequency region, the model is very accurate (Fig. 4b). The gain for the PPF filter is chosen by drawing the root locus and choosing the point where the damping in the filter pole is approximately equal to the damping in the first torsional mode.[9] For the parameter values listed in Table 1, a gain of 1.6 increases the nominal damping ratio of the first mode to 4.91% critical, a tenfold increase over the open loop.

Design of the Pointing Controller

Objectives for the slewing maneuver are stated in terms of the step response of the frame's hub position, as well as the maximum voltage of the control input. Formally, these are: minimize the overshoot, settling time, and steady-state error of the step response, a maximum control voltage of ± 5 V, and maximum controller size (including PPF compensator) of 15 states.

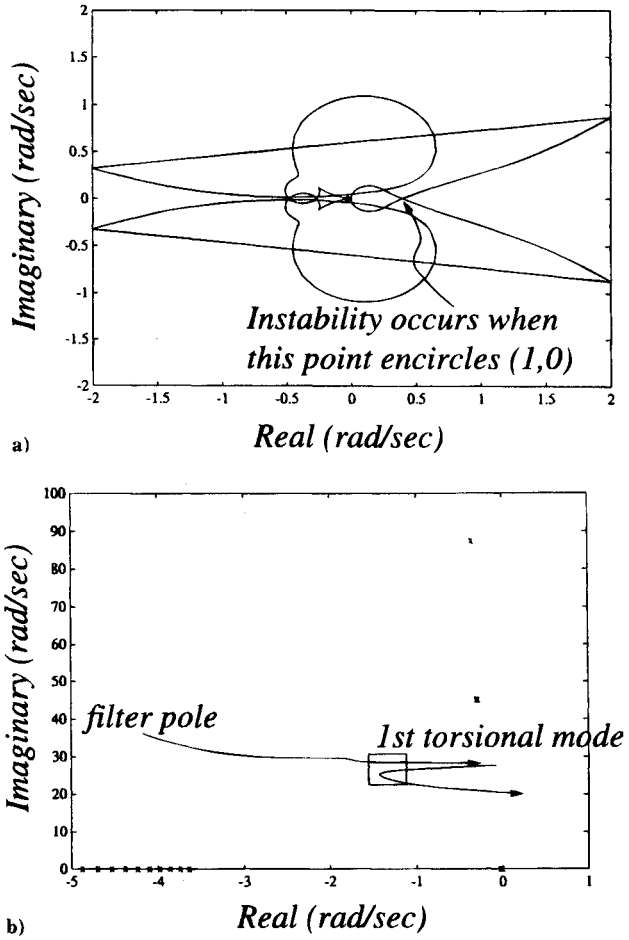

Fig. 5 Design of the PPF filter: a) a Nyquist plot illustrating the gain margin of the system and b) the root locus showing the movement of the closed-loop poles; the nominal design region is enclosed in a square box.

The final objective is due to the limits on the digital controller used in the experiments. It is an important requirement since it severely constrains the size of the model used for the control system design. In the case of μ synthesis, the order of the compensator is at least as great as the order of the model, so it is apparent that the order of the nominal model must be limited to approximately 10 or 12 states. Initially, Hankel model reduction is attempted on the system used for the PPF design. The order of this system is 45: 43 states comprise the open-loop dynamics, and the remaining states result from closing the PPF control loop. Numerical experiments show that the accuracy in the low-frequency region is severely degraded for models with less than 25 states, therefore a more ad hoc reduction scheme is performed. With the PPF control loop closed, the system has one input, the control voltage, and two outputs, the potentiometer and tachometer. Analytical transfer functions are obtained for each of these input/output relationships. Each transfer function is then truncated to include only the first five flexible modes. A balanced model is formed by expanding each transfer function into poles and residues, building a state-space system with complex entries. A coordinate transformation is then performed to make all of the entries real valued.[10] Although the final model is not based on physical coordinates, it is of low order (16 states) and maintains adequate accuracy in the low-frequency region.

Uncertainty Description

The next step in the controller design to determine a model for the uncertainty that exists in the system. For this paper, a multiplicative uncertainty at the potentiometer and tachometer outputs is assumed. Uncertainty bounds are acquired by com-

paring experimental transfer functions of the system $G_{exp}(s)$ to the nominal model $G_{nom}(s)$. The magnitude of the uncertainty is calculated from the expression

$$\frac{|G_{nom}(s) - G_{exp}(s)|}{|G_{nom}(s)|} \tag{10}$$

Due to the difficulty of obtaining experimental transfer functions between the control input and the potentiometer, only the uncertainty bound for the tachometer is calculated. Large peaks occur in the uncertainty due to the error in the natural frequencies of the model (Fig. 6).

To minimize the conservativeness of the compensator design, the uncertainty model is taken as an average value of the error between the experimental and nominal transfer functions. The uncertainty function, in the Laplace variable s, is given by:

$$W_{unc} = 0.35\,\frac{s/6\pi + 1}{s/1000 + 1} \tag{11}$$

Since the structured singular value μ is the test for stability robustness, it is also necessary to choose a structure for the uncertainty. To once again limit the conservativeness of the design, it is assumed that there is no correlation between uncertainty in the tachometer and potentiometer outputs. Therefore, the structure of the uncertainty block is

$$\Delta_u = \text{diag}[\Delta_{pot}\ \Delta_{tach}] \tag{12}$$

where the entries are individual 1×1 complex blocks. The final model for the uncertainty in the nominal model is shown in Fig. 7.

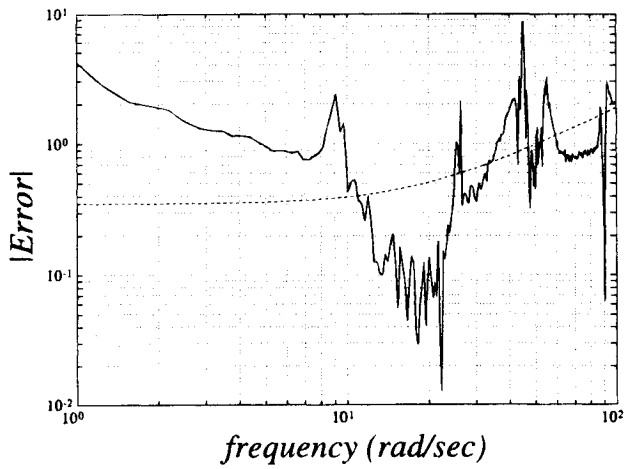

Fig. 6 Multiplicative error in the tachometer output (solid) and the corresponding uncertainty weight (dotted) for the robust stability analysis.

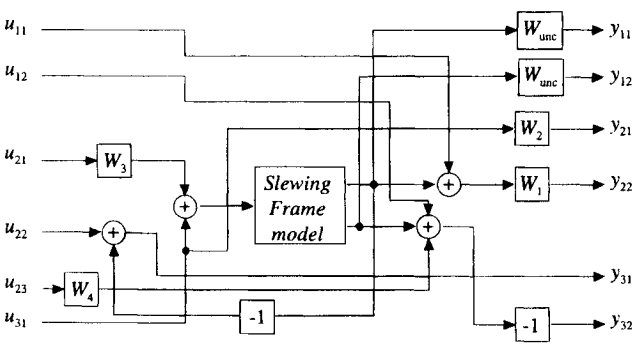

Fig. 7 Augmented plant used for μ synthesis design.

Determining a suitable uncertainty model for the robust control design is difficult due to the tradeoffs that exist in choosing the error functions. It is important to make the error set large enough so that the design is robust, but not too large so that it is unnecessarily conservative. Whether or not this assumption is valid is determined by the results. If the control system exhibits stability problems, it might be necessary to make the uncertainty model more conservative. The same is true for choosing the structure of the uncertainty. To make a less conservative design, the uncertainty in each channel is initially assumed to be uncorrelated. If this results in stability problems, the structure could be changed to a full 2×2 uncertainty block, making the robustness test a standard singular value plot of $M_{22}(s)$ [see Fig. 2 and Eq. (9)].

Robust Compensator Design Using μ Synthesis

The robust control technique μ synthesis involves augmenting the plant $P(s)$ with frequency-dependent functions that weight the various performance objectives. These performance weights are used to tradeoff between conflicting requirements, for example, low control effort vs quick response time. The choice of these weighting functions directly affects the design of the controller. Minimizing the number of functions used in the design is also important, because the size of the controller is always equal to or greater than the size of the augmented plant. The augmented plant for the μ synthesis is shown in Fig. 7.

For the slewing frame, closed-loop performance is shaped by the choice of four weighting functions, each corresponding to a specific performance objective. The first function, $W_1(s)$, weights the position response and is chosen to be a lead filter. Increasing the gain reduces the overshoot of the step response and making the numerator time constant larger speeds up the system. The second weight relates to the actuator effort. It increases at higher frequencies to force the controller to roll off. The function $W_3(s)$ is related to steady-state disturbance attenuation. Increasing the gain forces the DC gain of the controller to rise, thereby reducing steady-state error. The final weight is related to noise attenuation in the velocity signal, and is chosen to be a relatively small number due to its small effect on the system. The structure of the performance weights is chosen to be a full 3×2 block so that the optimization procedure accounts for the design tradeoffs. Using a block structure that does not couple the performance weights produces a less satisfactory design.

$$W_1(s) = 0.98\frac{s/2\pi + 1}{s/10 + 1}, \qquad W_2(s) = 0.3\frac{s/5\pi + 1}{s/10000 + 1}$$
$$W_3(s) = \frac{3}{s/0.002 + 1}, \qquad W_4 = .01 \tag{13}$$

The compensator design proceeds in the following manner. First, parameters for the performance weights are chosen and an H_∞ optimization is performed. If the ∞-norm of $M(s)$ is too large (> 20), this could indicate that the weights represent an unrealistic design and a more suitable set of weights should be chosen. If the norm is sufficiently small, the robust stability and performance measures [Eq. (9)] are plotted and the nominal time responses of the system are examined. If these are not satisfactory, an iterative procedure begins to reduce the maximum value of the structured singular value, thereby achieving a more robust design. This process, known as D-K iteration, involves first fitting a set of rational functions to the D scales of the closed-loop system matrix, $M(s)$. Once these functions are found, a state-space model is found for the system $D(s)P(s)D^{-1}(s)$ and another H_∞ optimization is performed on the transformed plant. This D-K iterative procedure is performed until a satisfactory design results.[7]

During the controller design for the slewing frame, a number of iterations on the weighting parameters are needed to achieve a satisfactory design. Plots of the weighting functions are shown

in Fig. 9a. The first H_∞ optimization achieved an ∞ norm of approximately 1.63, with robust stability being satisfied but not robust performance (Figs. 8a and 8b). Therefore, a *D-K* iteration is performed to reduce the maximum structured singular value. After the initial iteration, robust stability is maintained and robust performance is almost achieved, with the maximum structured singular value being 1.31. Further iterations do not reduce this value appreciably. Judging by the simulated time responses (Fig. 10), this design is considered satisfactory. Since robust stability is achieved and performance is robust as possible (i.e., the maximum value of μ cannot be reduced), this compensator is implemented on the slewing frame. The algorithms used in the control design are from the Musyn toolbox available from MATLAB.[8]

After the robust control design, the compensator has one output, two inputs, and 29 states. Hankel model reduction is used to decrease the compensator to 11 states with only a negligible effect on the dynamics. A magnitude plot of the reduced order compensator is shown in Fig. 9b. As expected, both channels roll off at higher frequencies and the low-frequency position gain is high. The roll-off characteristics are important for the robustness of the compensator, because they make the control law less sensitive to uncertainty at high frequencies. The high DC position gain is effective in reducing the steady-state error due to static friction and offsets in the hardware.

Experimental Results

Pointing control and vibration suppression is experimentally verified by implementing the robust compensator and PPF controller on the slewing frame. The frame is slewed by inputting a constant voltage into the motor which commands the structure to perform a 20-deg slewing maneuver. The hub position of the frame is measured using the potentiometer and the structural vibrations are measured using the output of active member 1. The control laws are implemented digitally using an Optima 3 processor sampling at 750 Hz. Numerical studies with the discrete time controller indicate that this sampling rate produces no degradation in closed-loop performance. Combining the pointing controller and supplementary PPF control yields a three input, two output control system with 13 states.

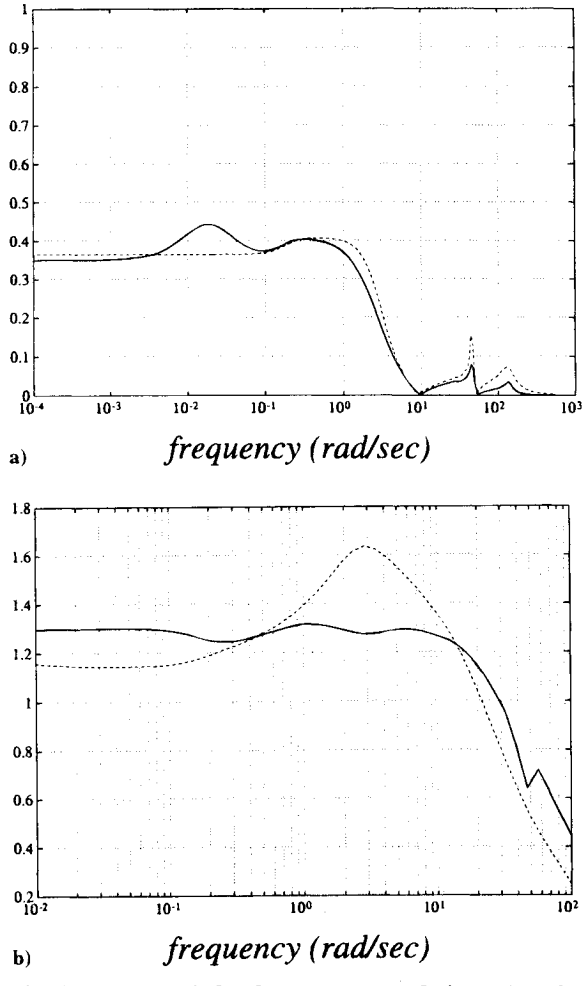

Fig. 8 Robust analysis for the compensator designs: a) μ plot for robust stability and b) μ plot for robust performance; the dotted line is after the first H_∞ optimization, the solid line is after the second.

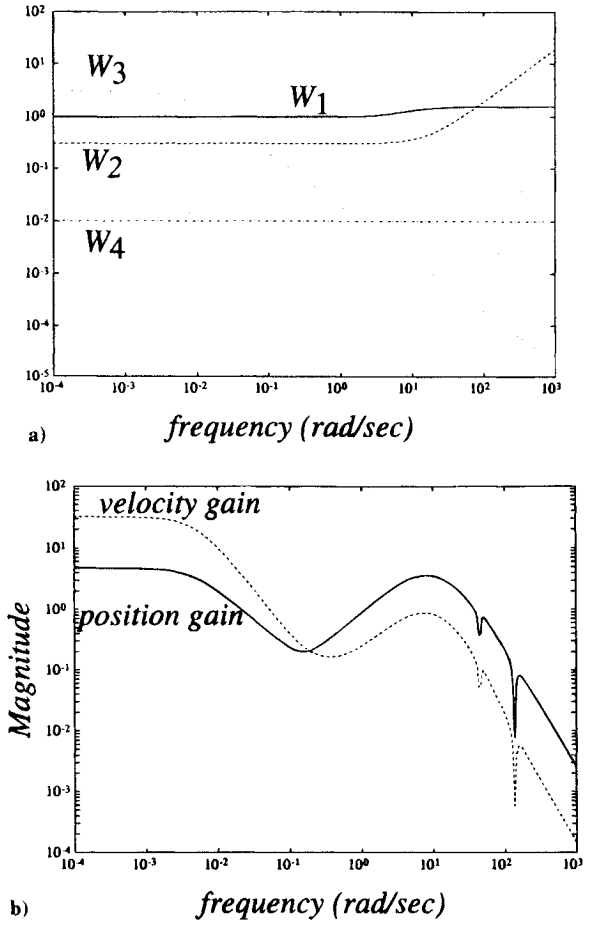

Fig. 9 a) Performance weights for the robust control design and b) magnitude plot of the final compensator design.

Table 2 Experimental results for the controller designed with μ synthesis

	Overshoot (%)	Settling time (s)	Steady-state error (%)
μ syn	7.0	2.0	<2.0

The results of the slewing experiment are illustrated in Fig. 11. The closed-loop step response of the hub position exhibits 7% overshoot, a 2-s settling time, and approximately 2% steady-state error due to static friction (Fig. 11a, Table 2). The structural vibrations due to the 20-deg slew are illustrated in Fig. 11b. Without the supplementary PPF control loop closed, the lightly damped torsional mode causes the frame to vibrate for over 30 s after the hub has come to rest. Closing the colocated PPF control loop reduces the settling time of the structural vibrations to only 4 s after the slew maneuver has ended. These results also indicate that the stability of the pointing controller is independent of the vibration suppression control loop, therefore it would maintain its performance if the active member happened

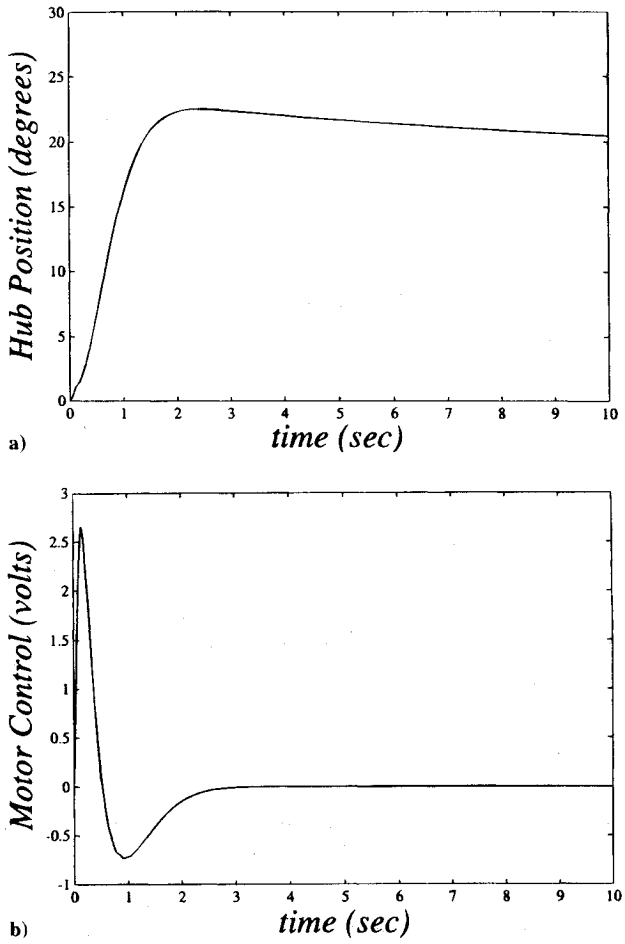

Fig. 10 Simulation results for the μ synthesis controller: a) hub position response to a step input and b) motor control voltage.

to fail. The maximum motor control effort of 2.6 V is well within the limit of ±5 V.

The experimental results show that the μ synthesis controller is robust in the presence of model uncertainty. No stability problems are encountered during the implementation of the μ compensator or PPF controller. These results are consistent with the robust stability analysis, which indicates that the control laws can tolerate the uncertainty that exists in the nominal model. Performance robustness is also achieved with respect to the assumed error. The experimental step response of the frame (Fig. 10) actually exhibits a smaller settling time and a slightly lower overshoot than the simulation. This is attributed to the damping that exists in the bearings and motor, which is not accounted for in the simulations.

Conclusions

Pointing control and vibration suppression in a slewing frame structure was achieved by designing two independent control laws. Vibration suppression of the first torsional mode was attained by using a piezoceramic active member in a colocated feedback loop. The PPF control law was robust against model error and increased the damping in the target mode by a factor of ten. The pointing control system was designed using μ analysis to maximize stability and performance robustness. Experimental results verified the effectiveness of the controller design. During a 20-deg slewing maneuver, the closed loop step response exhibited only a 7% overshoot, 2-s settling time, and less than 2% steady-state error. Without the supplementary PPF control, the frame vibrated for over 30 s after the end of the slewing maneuver. With the PPF control loop closed, the structural vibrations were suppressed 4 s after the hub position came to rest. Thus, slewing control and vibration suppression

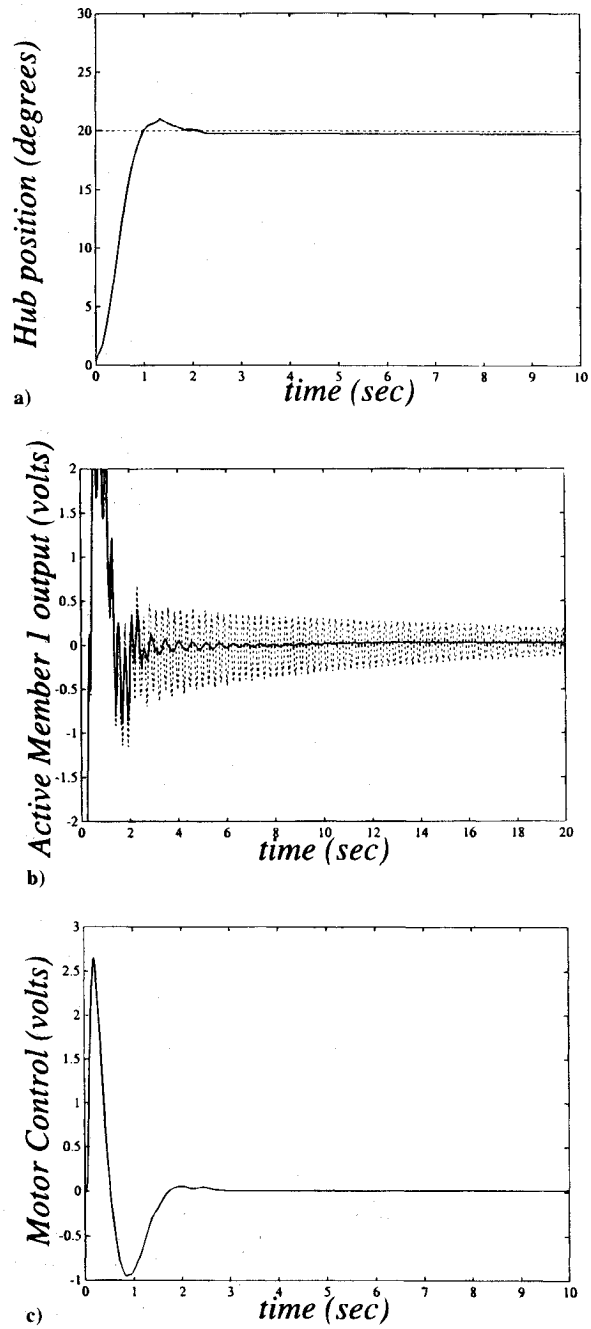

Fig. 11 Experimental results for μ synthesis controller: a) step response with 7% overshoot, 2-s settling time, and 2% steady-state error, b) structural vibrations induced during the maneuver without PPF control (dotted) and with PPF control (solid), and c) motor control voltage.

was achieved by using robust control laws in multiple feedback loops.

Acknowledgments

This work is funded by Air Force Office of Scientific Research grant number 910181 under the direction of Spencer Wu. The support is gratefully appreciated.

References

[1]Garcia, E., "On the Modeling and Control of Slewing Flexible Structures," Ph.D. Dissertation, Dept. of Mechanical and Aerospace Engineering, State Univ. of New York at Buffalo, Buffalo, NY, August, 1989.

[2]Juang, J. N., Horta, L. G., and Robertshaw, H. H., "A Slewing Control Experiment for Flexible Structures," *Journal of Guidance, Control, and Dynamics*, Vol. 9, No. 5, 1986, pp. 599–607.

[3] Junkins, J. L., Rahman, Z., and Bang, H., "Near-Minimum-Time Maneuvers of Flexible Vehicles: A Lyapunov Control Law Design Method," *Mechanics and Control of Large Flexible Structures*, edited by J. L. Junkins, Vol. 129, Progress in Astronautics and Aeronautics, AIAA, Washington, DC, 1990, pp. 565–593.

[4] Leo, D. J., and Inman, D. J., "Control of a Flexible Frame in Slewing," *Proceedings of the American Control Conference* (Chicago, IL), American Automatic Control Council, Evanston, IL. 1992, pp. 2535–2539.

[5] Leo, D. J., and Inman, D. J., "Modeling and Control Simulations of a Slewing Frame containing Active Members," *Smart Materials and Structures Journal* (2) 1993: pp. 82–95.

[6] Goh, C. J., and Caughey, T. K., "On the Stability Problem Caused by Finite Actuator Dynamics in the Colocated Control of Large Space Structures," *International Journal of Control*, Vol. 41, No. 3, 1985, pp. 787–802.

[7] Stein, G., and Doyle, J. C., "Beyond Singular Values and Loop Shaping," *Journal of Guidance, Control, and Dynamics*, Vol. 14, No. 1, 1991, pp. 5–15.

[8] Balas, G. J., Doyle, J. C., Glover, K., Packard, A., and Smith, R., *μ-Analysis and Synthesis Toolbox*, The Math Works, Inc., 1991.

[9] Fanson, J. L., and Caughey, T. K., "Positive Position Feedback Control for Large Space Structures," *Proceedings of the 28th Structures, Structural, Dynamics, and Materials Conference*, AIAA, Washington, DC, 1987, pp. 588–598.

[10] Crassidis, J. L., Leo, D. J., and Mook, D. J., "Experimental Verification of H_∞ Control on a Flexible Frame," *Proceedings of the Guidance, Navigation, and Control Conference* (Hilton Head, SC), AIAA, Washington, DC, 1992, pp. 106–115.